UCLA
UCLA Previously Published Works

Title

Ca2+ Signaling Augmented by ORAI1 Trafficking Regulates the Pathogenic State of Effector T Cells.

Permalink

https://escholarship.org/uc/item/0rn4112z

Journal

The Journal of Immunology, 208(6)

ISSN

0022-1767

Authors

Wu, Beibei
Woo, Jin Seok
Sun, Zuoming
et al.

Publication Date

2022-03-15

DOI

10.4049/jimmunol.2100871

Peer reviewed

eScholarship.org Powered by the California Digital Library
University of California

Author Manuscript

Author Manuscript

Author Manuscript

Author Manuscript

HHS Public Access

Author manuscript

J Immunol. Author manuscript; available in PMC 2023 March 15.

Published in final edited form as:

J Immunol. 2022 March 15; 208(6): 1329–1340. doi:10.4049/jimmunol.2100871.

Ca^{2+} signaling augmented by ORAI1 trafficking regulates the pathogenic state of effector T cells

Beibei Wu[*], **Jin Seok Woo**[*], **Zuoming Sun**[†], **Sonal Srikanth**[*,‡,¶], **Yousang Gwack**[*,‡,¶]

[*]Department of Physiology, David Geffen School of Medicine, University of California, Los Angeles, CA 90095, USA

[†]Department of Molecular Imaging & Therapy, Beckman Research Institute of City of Hope, Duarte, CA 91010, USA

Abstract

Activation of the Ca^{2+} release-activated Ca^{2+} (CRAC) channel is crucial for T cell functions. It was recently shown that naked cuticle homolog 2 (NKD2), a signaling adaptor molecule, orchestrates trafficking of ORAI1, a pore subunit of the CRAC channels, to the plasma membrane for sustained activation of the CRAC channels. However, the physiological role of sustained Ca^{2+} entry via ORAI1 trafficking remains poorly understood. Using NKD2 as a molecular handle, we show that ORAI1 trafficking is crucial for sustained Ca^{2+} entry and cytokine production, especially in inflammatory Th1 and Th17 cells. We find that murine T cells cultured under pathogenic Th17-polarizing conditions have higher Ca^{2+} levels that are NKD2-dependent than those under non-pathogenic conditions. In vivo, deletion of *Nkd2* alleviated clinical symptoms of experimental autoimmune encephalomyelitis (EAE) in mice by selectively decreasing effector T cell responses in the central nervous system. Furthermore, we observed a strong correlation between NKD2 expression and pro-inflammatory cytokine production in effector T cells. Together, our findings suggest that the pathogenic effector T cell response demands sustained Ca^{2+} entry supported by ORAI1 trafficking.

Introduction

Engagement of T cell receptors with cognate antigens depletes endoplasmic reticulum (ER) Ca^{2+} stores and triggers store-operated Ca^{2+} entry (SOCE). A specialized class of store-operated Ca^{2+} (SOC) channels, Ca^{2+} release-activated Ca^{2+} (CRAC) channels play a major role in elevation of intracellular Ca^{2+} concentration ($[Ca^{2+}]$) in T cells (1, 2). CRAC

[¶]Address correspondence to: Dr. Sonal Srikanth or Dr. Yousang Gwack, Department of Physiology, David Geffen School of Medicine, 53-266 CHS, 10833 Le Conte Avenue, Los Angeles, CA 90095, Tel: 310-794-2003; FAX: 310-206-5661, ssrikanth@mednet.ucla.edu; ygwack@mednet.ucla.edu.

[‡]Senior authors

AUTHOR CONTRIBUTIONS

Y.G. and S.S. designed and supervised research. S.S. performed Ca^{2+} imaging analysis. B.B.W. performed most of the biochemistry and flow cytometry experiments with primary T cells, characterized T cell phenotypes in *Nkd2*$^{-/-}$ mice, and performed in vivo experiments with help from J.S.W. Z.S. provided advice on the experimental procedures for EAE induction and manuscript preparation. Y.G. and S.S. wrote the manuscript with input from other authors.

COMPETING FINANCIAL INTERESTS

The authors do not have any competing financial interests.

Author Manuscript Author Manuscript Author Manuscript Author Manuscript

channels consist of the plasma membrane (PM)-localized pore subunit, ORAI1, and an ER Ca^{2+} sensor, stromal interaction molecule 1 (STIM1). STIM1 senses depletion of the ER Ca^{2+} stores and opens ORAI1. High and sustained Ca^{2+} signaling mediated by the CRAC channels is crucial for the induction of transcriptional programs via the NFAT (nuclear factor of activated T cells) pathway (1, 2). CRAC channels regulate various aspects of T cell biology, including their development, proliferation, differentiation, and cytokine production (1, 2). Inhibition of the core subunits of CRAC channels, ORAI1 and STIM1, can have pleiotropic effects, impeding the therapeutic exploitation of this pathway. Therefore, it is important to identify a cell type-specific mechanism underlying the regulation of CRAC channels, if any, for the design of targeted therapeutic strategies without systemic influence on T cell development or differentiation.

The current paradigm of CRAC channel activation emphasizes the crucial role of the interaction between ORAI1 and STIM1 for channel gating. However, multiple studies have reported the presence of ORAI1 in intracellular vesicles. Internalization of ORAI1 through vesicle trafficking by Rab5, caveolin, and dynamin mediates inhibition of SOCE during meiosis (3, 4). Furthermore, it was shown that only ~40% of ORAI1 localizes to the plasma membrane in cell-lines, and enrichment of ORAI1 at the plasma membrane after store depletion is passively achieved by trapping re-cycling ORAI1 by STIM1 (5). In a recent study, we identified naked cuticle homolog 2 (NKD2), a component of intracellular vesicles, as a vital regulator of CRAC channels that mediates trafficking of intracellular $ORAI1^{+}$ vesicles to the PM in effector T cells (6). Our data showed that TCR stimulation induces the insertion of $ORAI1^{+}$ vesicles into the PM in an NKD2-dependent manner. Using pH-sensitive GFP-tagged ORAI1, we demonstrated the insertion of $Orai1^{+}$ vesicles to the PM in a TCR stimulation-dependent manner, which was profoundly impaired in NKD2-deficient cells. Further, NKD2-mediated insertion of intracellular ORAI1 to the PM was dependent on protein kinase C (PKC) and Ca^{2+} signaling pathways. Deletion of *NKD2* impaired surface insertion of $ORAI1^{+}$ vesicles, SOCE, and cytokine production in primary human T cells. However, the detailed physiological role of NKD2-mediated ORAI1 trafficking in the effector T cell responses remains unexplored.

Experimental autoimmune encephalomyelitis (EAE) is a widely-used animal model for multiple sclerosis - a T cell-mediated demyelinating autoimmune disease in humans. Pathogenesis of EAE occurs in multiple steps. Naïve T cells get primed, proliferate, and differentiate to effector T cells in the lymph nodes after immunization. Effector Th1 and Th17 cells migrate to the central nervous system (CNS), where they encounter milieu enriched in self-antigen, cytokines, and local cellular factors (7). After re-stimulation in the inflamed tissue, effector T cells produce inflammatory cytokines, including IFN-γ, IL-17A, and GM-CSF, to recruit and activate microglia and macrophages. After infiltration into the CNS, Th17 cells trans-differentiate to Th1-like cells and become more pathogenic (8, 9). Intermediate IFN-γ^{+}IL-17A^{+} cells or completely converted IFN-γ^{+} ex-Th17 cells produce high levels of GM-CSF, a cytokine essential for EAE pathogenicity (8-11). Trans-differentiation of Th17 cells requires strong TCR signaling triggered by their encounter with self-antigen, polarizing cytokines (e.g., IL-12), and local cellular factors (e.g., serum amyloid A3) produced by tissue-resident cells that regulate expression of retinoid-related orphan receptor gamma t (RORγt), T-bet, Runx1, and Runx3 (12-14). In our previous work,

Author Manuscript Author Manuscript Author Manuscript Author Manuscript

we identified CRACR2a (CRAC channel regulator 2a) as an essential regulator of CRAC channels by stabilizing ORAI1-STIM1 interaction (15, 16). We showed that CRACR2a is expressed at high levels in effector T cells compared to naïve T cells, and deletion of *Cracr2a* selectively blocks Th1 and Th17 responses only in the inflamed tissues without influencing the priming phase of T cells in the lymph nodes (17). These results suggest that while CRAC channels are expected to play a broad role in general T cell functions, effector T cells in the inflamed tissue may exert a unique molecular program to support a robust and sustained intracellular Ca^{2+} increase, which is required for inflammatory cytokine production by Th1 cells and trans-differentiation of Th17 cells.

In this study, using NKD2 as a molecular handle, we systematically show that ORAI1 trafficking is crucial for sustained Ca^{2+} entry and the effector functions (e.g., cytokine production) in inflammatory Th1 and Th17 cells. Using in vitro T cell culture, we find that NKD2 is abundantly expressed in inflammatory T cells and contributes to their higher Ca^{2+} levels. In vivo, deletion of *Nkd2* did not affect T cell development and homeostasis under sterile conditions, and priming in the lymph nodes after immunization. However, *Nkd2* deletion alleviated clinical symptoms of EAE by selectively decreasing effector T cell responses in the CNS. Furthermore, we observed a strong correlation between NKD2 expression and cytokine levels in effector T cells from the CNS. Together, our findings suggest that sustained Ca^{2+} entry supported by ORAI1 trafficking is a requirement for the pathogenic effector T cell responses.

Material and Methods

Chemicals and antibodies.

Fura 2-AM (F1221) and brefeldin A were purchased from Thermofisher Scientific. Antibody for detection of mouse NKD2 (2596) was purchased from Cell Signaling Technologies. Antibody for detection of β-actin (sc-47778) was obtained from Santa Cruz Biotechnology.

Mice.

Nkd2$^{-/-}$ mice were purchased from The Jackson Laboratory (stock #006960). 8-10-week-old age- and sex-matched control (*Nkd2*$^{+/+}$) and *Nkd2*$^{-/-}$ littermate animals were used for all in vivo experiments. For in vitro T cell culture 6-8-week-old mice with age- and sex-matched controls were used. For passive EAE experiments, age-matched donor and *Rag2*$^{-/-}$ recipients (purchased from The Jackson Laboratory, stock #008449) were used. All animals were maintained in pathogen-free barrier facilities and used following protocols approved by the Institutional Animal Care and Use Committee at the University of California, Los Angeles.

Immunoblotting.

For immunoblot analyses, cells were lysed in RIPA buffer (10 mM Tris-Cl pH 8.0, 1% Triton X-100, 0.1% SDS, 140 mM NaCl, 1 mM EDTA, 0.1% sodium deoxycholate and protease inhibitor cocktail [Roche]) and centrifuged to remove debris. Samples were separated on 8-10% SDS-PAGE. Proteins were transferred to nitrocellulose membranes

Author Manuscript Author Manuscript Author Manuscript Author Manuscript

and subsequently analyzed by immunoblotting with relevant antibodies. Chemiluminescence images were acquired using an Image reader LAS-3000 LCD camera (FujiFilm).

RNA isolation, cDNA synthesis and real-time quantitative PCR.

Total RNA from cells harvested in TRIzol Reagent (Thermofisher Scientific) was isolated using the Direct-zol RNA isolation kit (Zymo Research). RNA quantity and quality were confirmed with a NanoDrop ND-1000 spectrophotometer. cDNA was synthesized using 1-2 μg of total RNA using oligo(dT) primers and Maxima Reverse Transcriptase (Thermofisher Scientific). Real-time PCR was performed using iTaq Universal SYBR Green Supermix (Bio-Rad) and an iCycler IQ5 system (Bio-Rad) using gene-specific primers described in Table S1. Threshold cycles (C_T) for all the candidate genes were normalized to those of 36B4 to obtain ΔC_T. The specificity of primers was examined by melt-curve analysis and agarose gel electrophoresis of PCR products.

Single-cell Ca^{2+} imaging.

Primary T Cells were loaded at 1 x 10^6 cells/ml with 1 μM Fura 2-AM for 30 min at 25°C and attached to poly-L-lysine–coated coverslips. Intracellular $[Ca^{2+}]_i$ measurements were performed using essentially the same methods as previously described (18).

Surface ORAI1 staining and analysis.

Naïve $CD4^+$ T cells isolated from control and *Nkd2*$^{-/-}$ animals were transduced with retroviruses encoding empty vector or plasmids encoding ORAI1- EC-HA (it expresses ORAI1 protein containing an HA tag in its second extracellular loop to allow for detection using surface staining), cultured under non-polarizing for four days, and were left untreated or stimulated with soluble anti-CD3 antibody (1 μg/ml) and cross-linked with goat anti-hamster antibody for indicated times. Cells were treated with anti-HA and secondary antibodies in PBS with 2% FBS on ice, subsequently, fixed with 4% paraformaldehyde (PFA) for 15 minutes at room temperature and analyzed with a FACSCalibur flow cytometer and FlowJo software.

T cell purification, stimulation, differentiation, and staining.

T cell purification, activation, and differentiation were carried out as previously described (17, 19). Briefly, naïve $CD4^+$ T cells were enriched by magnetic sorting from single-cell suspensions generated by mechanical disruption of spleens and lymph nodes of adult mice using MagniSort naïve $CD4^+$ T cell enrichment kit (catalog # 8804-6824-74, ThermoFisher Scientific). For effector T cell differentiation, cells were stimulated with 1 μg/ml of anti-CD3 antibody (1452C11, Bio X Cell) and 1 μg/ml of anti-CD28 antibody (Clone 37.51, Bio X Cell) for 48 hours on a plate coated with 0.3 mg/ml of rabbit anti-hamster antibody (MP Biomedicals). $CD4^+CD25^-$ T cells were cultured without any polarizing cytokines or antibodies for non-polarizing (ThN) conditions, with 10 μg/ml anti-IL-4 antibody (Peprotech) and 10 ng/ml IL-12 for Th1 differentiation; 20 μg/ml anti-IFN-γ antibody (Bio X Cell), 2.5 μg/ml anti-IL-12 antibody and 10 ng/ml IL-4 for Th2 differentiation; 10 μg/ml anti-IL-4 antibody, 10 μg/ml anti-IFN-γ antibody, 30 ng/ml IL-6 (Peprotech) and 1 ng/ml TGF-β (Peprotech) for non-pathogenic Th17 differentiation; 10 μg/ml anti-IL-4

Author Manuscript Author Manuscript Author Manuscript Author Manuscript

antibody, 10 μg/ml anti-IFN-γ antibody, 30 ng/ml IL-6 (Peprotech), 10 ng/ml IL-23 (R&D Systems) and 10 ng/ml IL-1β (R&D Systems) for pathogenic Th17 differentiation. On day 4, differentiated T cells were re-stimulated with 1 μg/ml of anti-CD3 antibody and 1 μg/ml of anti-CD28 antibody for 5 hours for cytokine analysis. Brefeldin A (1 μg/ml) was added for the last 2 hours. Cells were harvested, washed in PBS, permeabilized with 0.5% saponin, and stained intracellularly for indicated cytokines. For staining of transcription factors, differentiated effector T cells were fixed/permeabilized and stained using Transcription Factor Staining Buffer Set (BD Pharmingen). For surface staining, 1 x 10^6 cells from single cell suspensions of thymus, spleen and lymph nodes were stained with indicated antibodies in PBS + 1% fetal bovine serum, at 4°C for 20 mins, washed and used for data acquisition immediately. For CTV Labeling experiment, naïve T cells were labeled using CellTrace™ Violet Cell Proliferation Kit according to the manufacturer's protocols. CTV-labeled control and *Nkd2*$^{-/-}$ naïve T cells were cultured under non-polarizing conditions and were harvested and analyzed by flow cytometry on day 4. Data were acquired using FACSCalibur (Becton Dickinson) or BD LSRFortessa cell analyzers and analyzed using FlowJo software (Tree Star). Most of the flow cytometry antibodies were purchased from ThermoFisher Scientific, including anti-IL-4-APC (11B11), anti-IL-17-APC (eBio17B7), anti-IFN-γ-PE (XMG1.2), anti-GM-CSF-FITC (MP1-22E9), anti-IL-10-PE, (JESS-16E3), anti-Foxp3-APC (FJK-16s), anti-T-bet-APC (4B10), anti-RORγT-PE (AFKJS-9), anti-CD4-PerCP (RM4-5), anti-CD8b-PE/PerCP (H35-17.2), anti-CD44-PerCP (IM7), anti-CD62L-APC (MEL-14), anti-CD25-APC (PC61.5), and anti-CD69-PerCP (H1.2F3). Anti-IL23R-PE (12B2B64) was purchased from BioLegend.

EAE induction and analyses.

For reconstitution of naïve T cells in *Rag2*$^{-/-}$ mice, 5 × 10^6 $CD4^+CD25^-$ T cells purified using MagniSort naïve $CD4^+$ T cell enrichment kit from *Nkd2*$^{+/+}$ and *Nkd2*$^{-/-}$ mice were transferred intraperitoneally into *Rag2*$^{-/-}$ mice, followed by active induction of EAE after 2 weeks (20). Mice were immunized subcutaneously on day 0 with 100 μg of $MOG_{35–55}$ peptide (N-MEVGWYRSPFSRVVHLYRNGK-C, Genscript) emulsified in complete Freund's adjuvant (CFA, Difco) supplemented with 5 mg/mL of *Mycobacterium tuberculosis* H37Ra (Difco) as previously described (17). The mice were also injected i.p. with pertussis toxin (200 ng/mouse, List Biological Laboratories) on days 0 and 2. For passive EAE, donor control (*Nkd2*$^{+/+}$) and *Nkd2*$^{-/-}$ mice were first immunized with $MOG_{35–55}$ subcutaneously as described above. At the first sign of EAE symptoms (score 0.5), draining lymph node cells were collected and cultured under Th17-expanding conditions with 20 ug/ml of $MOG_{35–55}$ peptide, IL-1β (10 ng/ml), and IL-23 (10 ng/mL) for 3 days. At day 3, 5 x 10^6 cells were injected intravenously into *Rag2*$^{-/-}$ mice. EAE severity was scored according to the following clinical scoring system: 0, no clinical signs; 1, paralyzed tail; 2, partial hind leg paralysis; 3, complete hind leg paralysis or partial hind and front leg paralysis; 4, complete hind and partial front leg paralysis.

Isolation and analysis of cells from the central nervous system in EAE-induced mice.

As previously described (17), mononuclear cells were isolated from spinal cords and brains; tissues were digested with collagenase and DNase I (Roche) for 30 min at 37°C, and cells were separated on a 40-80% Percoll gradient by centrifugation at 500 g for 30 minutes. Cells

Author Manuscript Author Manuscript Author Manuscript Author Manuscript

at the 40-80% interface were collected. Cells were also isolated from draining lymph nodes by passing through nylon mesh, followed by lysis of blood cells and washing with PBS. For intracellular cytokine staining, cells were stimulated with 80 nM PMA and 1 μM ionomycin in the presence of 3 μg/ml brefeldin A for 5 hours and stained with antibodies for detection of CD4, IFN-γ, IL-17A, GM-CSF, and NKD2.

Statistical analysis.

Statistical analysis was carried out using two-tailed Student's t-test. Differences were considered significant when p values were <0.05. For EAE clinical score measurements, statistical significance was calculated using the Mann-Whitney U test.

Results

Normal T cell development and homeostasis in *Nkd2* knockout mice

To examine the physiological role of NKD2 in T cell functions, we analyzed T cell phenotypes of $Nkd2^{-/-}$ mice. Consistent with a previous publication (21), $Nkd2^{-/-}$ mice were fertile and did not show anomalies in their litter size, survival, and body weight, compared to age and sex-matched littermate controls. Further, numbers and frequencies of $CD4^+$ and $CD8^+$ T cells in the thymi, spleens, and lymph nodes of $Nkd2^{-/-}$ mice were comparable to control animals, indicating normal development and homeostatic growth of T cells (Figs. 1A, B, and Suppl. Fig. 1A). Also, steady-state T cell activation levels in the spleen and lymph nodes were similar between control and $Nkd2^{-/-}$ mice when judged by surface expression of CD62L, CD44, CD25, and CD69 (Suppl. Figs. 1B and C). FoxP3 expression was also similar between control and $Nkd2^{-/-}$ $CD4^+$ T cells isolated from the thymus, spleen, and lymph nodes (Fig. 1C). These results collectively suggest that loss of *Nkd2* does not affect development and homeostasis of conventional and regulatory T cells.

Abundant expression of NKD2 in inflammatory effector T cells

Next, we examined the expression of NKD2 among naïve and different effector T cell populations. Among effector T cells, Th17 cells display great diversity in their function. Th17 cells differentiated with TGF-β1 + IL-6 are poor inducers of inflammation and considered non-pathogenic, while those cultured in the presence of IL-1β + IL-6 + IL-23 or TGF-β1 + IL-6 + IL-23 show enhanced expression of inflammatory cytokines and are considered pathogenic that elicit EAE with severe tissue damage (22-24). Flow cytometric examination of NKD2 expression showed that effector cells expressed much higher levels of NKD2 when compared to naïve T cells (Fig. 2A). $Nkd2^{-/-}$ cells were used as negative controls in these experiments. Among Th17 cells, we found that NKD2 expression was elevated in T cells cultured under pathogenic Th17-polarizing conditions (IL-1β + IL-6 + IL-23) compared to those under non-pathogenic Th17-polarizing conditions (TGF-β1 + IL-6). These observations were also confirmed by quantitative analysis of *Nkd2* transcripts (Fig. 2B). Next, we validated these results with immunoblotting. We observed higher expression of NKD2 in primary T cells cultured under non-polarizing, Th1-, and pathogenic Th17-polarizing conditions than those cultured under Th2- and Treg-polarizing conditions (Fig. 2C). Previously, we detected enhanced surface expression of ORAI1 upon TCR stimulation in human T cells expressing ORAI1 protein with an HA

Author Manuscript Author Manuscript Author Manuscript Author Manuscript

tag inserted in its second extracellular loop. Surface staining of these cells using anti-HA antibodies allowed for detection of PM-resident ORAI1 (6). Using the same technique, murine effector T cells transduced for expression of extracellular HA-tagged ORAI1 and cultured under non-polarizing conditions (predominantly Th1 cells) also showed enhanced surface expression of ORAI1 upon TCR stimulation, which was reduced in *Nkd2*$^{-/-}$ effector T cells (Fig. 2D). Since NKD2 expression was higher in T cells cultured under pathogenic Th17-polarizing conditions (Fig. 2A), we compared levels of surface ORAI1 insertion between T cells cultured under pathogenic and non-pathogenic Th17-polarizing conditions. Our analysis showed increased ORAI1 insertion into the plasma membrane in T cells cultured under pathogenic Th17-polarizing conditions compared to those under non-pathogenic Th17-polarizing conditions, which were decreased by the loss of NKD2 (Fig. 2E). These data show the conserved function of NKD2 in stimulation-induced surface expression of ORAI1 in inflammatory T cells.

NKD2 is crucial for Ca^{2+} signaling and cytokine production in effector T cells

We found that *Nkd2*$^{-/-}$ thymocytes and naïve T cells did not show any impairment in SOCE, in consistence with its minimal role in T cell development and homeostasis (Figs. 3A and B). However, *Nkd2*$^{-/-}$ effector T cells cultured under non-polarizing conditions showed reduced SOCE compared to wild-type cells (Fig. 3C). Measurement of SOCE in T cells cultured under Th17-polarizing conditions led to two interesting findings. First, T cells cultured under pathogenic Th17-polarizing conditions showed significantly higher SOCE than those under non-pathogenic Th17-polarizing conditions when triggered by TCR stimulation (Fig. 3D). Second, loss of NKD2 reduced SOCE in T cells cultured under pathogenic Th17-polarizing conditions, whereas those cultured under non-pathogenic conditions showed normal SOCE. Consistent with SOCE measurements, we observed a decrease in expression of IFN-γ in *Nkd2*$^{-/-}$ effector T cells cultured under non-polarizing conditions without affecting their proliferation (Fig. 3E and Suppl. Fig. 2). In consistence with our SOCE measurements with Th17 cells, IL-17A expression was reduced in *Nkd2*$^{-/-}$ cells differentiated only under pathogenic Th17-polarizing conditions but not under non-pathogenic Th17-polarizing conditions (Fig. 3E). IL-4 and Foxp3 expression in T cells cultured under Th2- and Treg-polarizing conditions were not influenced by *Nkd2* deletion. In all these experiments T cells were stimulated with anti-CD3 and anti-CD28 antibodies because we previously showed that TCR and co-receptor signaling pathways synergistically activate NKD2 to induce ORAI1 trafficking while treatment with chemical agonists, including PMA and ionomycin, that bypass TCR signaling, had a minor effect on ORAI1 trafficking (6). Furthermore, transcript analysis showed reduced expression of *Il17a* and *Il17f* only in T cells cultured under pathogenic Th17-polarizing conditions (Fig. 3F), suggesting SOCE-mediated regulation of transcription of IL-17.

Normal expression of RORγt and RORα but reduced levels of T-bet, GM-CSF, and IL-23R in *Nkd2* KO Th17 cells

To exclude the possibility that IL-17 expression in *Nkd2*$^{-/-}$ cells was impaired due to their failure in differentiation, we assessed the expression of key transcription factors necessary for Th17 differentiation (25, 26). *Nkd2*$^{-/-}$ T cells cultured under non-pathogenic and pathogenic Th17-polarizing conditions did not show any difference in mRNA and protein

Author Manuscript Author Manuscript Author Manuscript Author Manuscript

expression levels of RORγt and RORα, signature transcription factors of Th17 (Figs. 4A and B). Of note, our previous data showed a comparable expression of T-bet in *NKD2* KO human primary T cells despite a severe defect in expressions of Th1 cytokines, including IFN-γ, TNF, and IL-2 (6). Collectively, normal expression of RORγt and RORα suggests that the early phase of naïve T cell differentiation into Th17 cells is intact potentially due to the low expression of NKD2 in naïve T cells (Fig. 2A).

Next, we examined expression of markers involved in pathogenicity and maintenance of Th17 cells in control and *Nkd2*$^{-/-}$ cells cultured under non-pathogenic or pathogenic Th17-polarizing conditions. T-bet was shown to be highly expressed in pathogenic Th17 cells and essential for pathogenicity of Th17 cells (12, 24, 27). Transcript analysis showed that mRNA expression in *Tbx21* is high in T cells cultured under non-polarizing conditions, mostly Th1 cells and in those cultured under pathogenic Th17-polarizing conditions (Fig. 4C). These data were supported by protein analysis, where protein levels of T-bet were reduced only in T cells cultured under pathogenic Th17-polarizing conditions, but not ThN or those cultured under non-pathogenic Th17-polarizing conditions (Fig. 4D). We also checked the expression levels of GM-CSF and IL-23 receptor (IL-23R) that are essential for pathogenicity of Th17 cells during the effector and maintenance phases, respectively (10, 11, 28). Their signaling pathways are connected because IL-23 signaling is important for production of GM-CSF in Th17 cells (10). Both mRNA and protein levels of GM-CSF and IL-23R were high in T cells cultured under pathogenic Th17-polarizing conditions, and their expression was reduced in *Nkd2*$^{-/-}$ cells (Figs. 4E and F). Collectively, these data suggest that NKD2 is not essential for the initial phase of Th17 differentiation judged by normal expression of RORγt and RORα, but *Nkd2*$^{-/-}$ Th17 cells can have defects in the later stages, including the effector and maintenance phases.

Conversion of Th17 cells into Th1-like cells after IL-12 treatment is impaired by NKD2 deficiency

So far, our data indicate that NKD2 is important for the late event of Th17 differentiation, including cytokine production and maintenance. We sought to validate this using in vitro Th17 conversion model by taking advantage of the finding that expression of signature cytokine and transcription factors is normal in *Nkd2*$^{-/-}$ T cells cultured under non-pathogenic Th17-polarizing conditions (Figs. 3E, 3F, 4A, and 4B). Th17 cells are plastic, and in the inflamed tissue, they are converted into Th1-like T cells (or IFN-γ^{+} ex-Th17) that express T-bet and produce IFN-γ as a terminal state (8, 27). Under in vitro conditions, re-stimulation of non-pathogenic Th17 cells in the presence of IL-12 supports their trans-differentiation to Th1-like cells mimicking the terminal event of Th17 cells in the inflamed tissue (12, 17). In this assay, control and *Nkd2*$^{-/-}$ T cells cultured under non-pathogenic Th17-polarizing conditions showed similar IL-17A expression, consistent with our previous observation (Fig. 5A). After re-stimulation in the presence of IL-12, control cells trans-differentiated into Th1-like cells expressing IFN-γ and T-bet, as reported previously (Fig. 5B) (8, 12, 27). Under both conditions of the absence and presence of IL-12, we found that *Nkd2*$^{-/-}$ cells exhibit impairment in transitioning to T cells expressing IFN-γ and T-bet. We also found reduced expression of transcripts of *Ifng*, *Tbx21*, *Runx1*, and *Runx3* in *Nkd2*$^{-/-}$ T cells cultured under the same conditions (Fig. 5C). These data

Author Manuscript Author Manuscript Author Manuscript Author Manuscript

collectively suggest that NKD2-dependent high and sustained SOCE supports the terminal event of Th17 cells, including their conversion into Th1-like cells.

Loss of NKD2 impairs local effector T cell functions without affecting their initial priming in the lymph nodes

Since outcomes from active EAE induction in *Nkd2*$^{-/-}$ mice can be influenced by global deletion of *Nkd2* in various cell types, to examine physiological role of *Nkd2*$^{-/-}$ T cells, we transferred control or *Nkd2*$^{-/-}$ CD4^{+}CD25^{-} naïve T cells into *Rag2*$^{-/-}$ mice. Consistently with the results from the analysis of global *Nkd2*$^{-/-}$ mice (Figs. 1A, 1B, and Suppl. Fig. 1A), CD4^{+} T cell numbers cell from spleen and lymph nodes of recipients prior to induction of EAE (two weeks post-transfer) were similar (Fig. 6A). As expected from the analysis of cultured T cells, recipients of *Nkd2*$^{-/-}$ T cells showed milder symptoms of EAE when compared to those of control T cells (Fig. 6B). Accordingly, recipients of *Nkd2*$^{-/-}$ T cells showed fewer numbers of total mononuclear cells and CD4^{+} T cells in the CNS. Consistent with the analysis of T cells cultured in vitro, cytokine analysis showed reduced expression of IFN-γ and IL-17A in cells isolated from the CNS of recipients of *Nkd2*$^{-/-}$ T cells (Fig. 6C). We also observed a significantly reduced frequency of IFN-γ^{+}IL-17A^{+} double-positive CD4^{+} T cells in the CNS of the recipients of *Nkd2*$^{-/-}$ T cells. This IFN-γ^{+}IL-17A^{+} double-positive subset is derived from Th17 cells and is known to contribute to the pathogenicity of Th17 cells in autoimmune diseases (8, 12, 27). GM-CSF has also been identified as a critical cytokine that contributes to the pathogenicity of inflammatory T cells in EAE by inducing activation and recruitment of innate immune cells (10, 11). In support of the analysis of clinical scores, we observed a significant decrease in the frequency of GM-CSF-producing Th1 and Th17 cells isolated from the CNS of the recipients of *Nkd2*$^{-/-}$ T cells compared to those of control T cells.

To determine whether the reduced clinical symptoms in recipients of *Nkd2*$^{-/-}$ T cells were due to impaired priming of Th1 and Th17 cells, we analyzed T cells isolated from the draining lymph nodes of EAE-induced WT and *Nkd2*$^{-/-}$ mice at the early stages of disease onset (day 10 after EAE induction). Interestingly, we did not observe any difference in expression of IFN-γ and IL-17A in *Nkd2*$^{-/-}$ T cells from the draining lymph nodes, when compared to WT controls (Fig. 6D). Further, transcript levels of various genes involved in Th1 (*Ifng, Tbx21, Itga4, Ccr5*, and *Cxcr3*) or Th17 (*Il17a, Rorc, Itgal, Ccr6,* and *Il23r*) responses were not affected due to loss of NKD2 (Fig. 6E). These results suggest that the decreased production of IFN-γ and IL-17 in T cells isolated from the CNS is unlikely due to impairment in priming of T cells.

In the inflamed tissue, Th17 cells trans-differentiate to Th1-like cells (8, 9). Intermediate IFN-γ^{+}IL-17A^{+} cells or completely converted IFN-γ^{+}IL-17A^{-} cells have high pathogenicity (8-11). Trans-differentiation of Th17 cells requires strong TCR signaling, including elevated Ca^{2+} levels, triggered by an encounter with self-antigens and cytokines produced by tissue-resident cells (e.g., IL-12) that induce expression of T-bet, Runx1, and Runx3 (12, 17). To further dissect the role of NKD2 specifically in Th17 cell functions at the site of inflammation, we carried out adoptive Th17 cell transfer-mediated EAE. Cells from the draining lymph nodes of EAE-induced control and *Nkd2*$^{-/-}$ mice cultured under Th17-

Author Manuscript Author Manuscript Author Manuscript Author Manuscript

expansion conditions (IL-1β + IL-23) for three days showed similar frequencies of IL-17A$^+$ T cells when stimulated with PMA and ionomycin treatment that bypasses proximal TCR signaling and activation of NKD2 (Fig. 7A). *Rag2*$^{-/-}$ recipients reconstituted with donor cells from WT and *Nkd2*$^{-/-}$ mice developed EAE with a similar onset time. However, the disease severity was significantly reduced in recipients of *Nkd2*$^{-/-}$ T cells compared with those of control cells (Fig. 7B). In support of these data, total mononuclear and CD4$^+$ T cell numbers were reduced in the CNS of recipients of *Nkd2*$^{-/-}$ T cells. A significant fraction of the transferred T cells transited to IFN-γ-producing cells, which was significantly reduced in the recipients of *Nkd2*$^{-/-}$ T cells (Fig. 7C), consistent with in vitro Th17 conversion model (Figs. 5B and C). Expression of GM-CSF was also significantly reduced in *Nkd2*$^{-/-}$ CD4$^+$ T cells. Consistent with our analysis of cytokine expression in the CNS, we observed a significant reduction in transcripts of *Tbx21*, *Runx1*, and *Runx3*, which are involved in pathogenicity of Th17 cells in the CNS of recipients of *Nkd2*$^{-/-}$ T cells (Fig. 7D). Expression of mRNAs of *Tcf7*, a transcription factor regulating the stem cell-like state of Th17 cells (29), was not influenced by NKD2 deficiency.

In addition to the functional consequences of NKD2 deficiency, we also observed a strong correlation between NKD2 expression and the inflammatory state of T cells. Using *Nkd2*$^{-/-}$ T cells as controls we identified NKD2$^+$ and NKD2$^-$ T cells among mononuclear cells isolated from the CNS (Fig. 8, left). Next, we checked the expression of IFN-γ, IL-17A, and GM-CSF in those cells (Fig. 8, right). These results showed increased cytokine expression in NKD2$^+$ cells than in NKD2$^-$ cells, validating correlation between NKD2 expression and the inflammatory state of T cells. Together, these results indicate that NKD2 plays an important role in Th17 pathogenicity by supporting SOCE and the terminal state (e.g., cytokine production, conversion) in the inflamed tissue.

Discussion

Three models of CRAC channel activation were previously proposed; the conformational coupling, diffusible messenger, and vesicle fusion models (30). The current paradigm of ORAI1-STIM1 coupling supports only the conformational coupling model by emphasizing the crucial role of the interaction between ORAI1 and STIM1 for channel gating. However, the other models also supported by experimental evidence have been largely neglected. Internalization of ORAI1 through vesicle trafficking by Rab5, caveolin, and dynamin mediates inhibition of SOCE during meiosis (3, 4). Furthermore, it was shown that only ~40% of ORAI1 localizes to the plasma membrane, and enrichment of ORAI1 at the plasma membrane after store depletion is passively achieved by trapping re-cycling ORAI1 by STIM1 (5). Our previous study showed that an active signaling mechanism triggered by TCR stimulation exists to traffic ORAI1 from the intracellular pool to the plasma membrane, which is mediated by NKD2 and essential for sustained Ca^{2+} signaling for a prolonged period (6). As a follow-up, in the current study using NKD2 as a molecular handle, we have identified a physiological role of ORAI1$^+$ vesicle trafficking, especially in the effector T cell responses at the inflamed tissue in autoimmunity.

Effector Th1 and Th17 cells are essential for tissue homeostasis and host defense against pathogens (31, 32). Conversely, these effector T cells can also be the culprits of various

Author Manuscript Author Manuscript Author Manuscript Author Manuscript

autoimmune disorders. Recent investigations focus on the mechanisms underlying the inflammatory state of effector T cells that cause tissue damage. These studies have so far identified a role for self-antigen, inflammatory cytokine milieu, and local cellular factors for the pathogenic conversion of effector T cells. Here we highlight that a unique cell-intrinsic mechanism mediated by NKD2, a vesicular protein that regulates ORAI1 trafficking, is essential for the local effector function of Th1 and Th17 cells. Our previous study showed that NKD2 acts as a signaling adaptor molecule that converts TCR signals to trafficking intracellular ORAI1 pool to the plasma membrane to support sustained Ca^{2+} entry (6). Importantly, this study revealed that loss of NKD2 impaired production of Th1 cytokines (e.g., IFN-γ, TNF, and IL-2) in human primary T cells without influencing expression of the signature transcription factor, T-bet. The current study using *Nkd2*$^{-/-}$ mice reveals that NKD2 is; *i)* abundantly expressed in Th1 and Th17 cells and essential for ORAI1-mediated Ca^{2+} influx in those cells, *ii)* crucial for the late events of Th17 cells, including cytokine production, expression of IL-23R, and trans-differentiation, and *iii)* not involved in the development, homeostatic growth, and priming of T cells but is essential for their local effector functions.

Several observations support our conclusion that the function of inflammatory T cells demands high and sustained Ca^{2+} signaling. Earlier studies using mice with deletion of *Orai1* and *Stim* genes, as well as blockers to block SOCE, have shown the critical role of SOCE in EAE (19, 33). T cell-specific loss of STIM proteins (both STIM1 and its homolog STIM2) rendered mice resistant to EAE (33). In agreement with our observations with *Nkd2*$^{-/-}$ T cells, loss of STIM proteins impaired production of proinflammatory cytokines and expression of IL-23R in encephalitogenic T cells, without influencing expression of signature transcription factors, RORγt and RORα (33). Inhibition of SOCE using an ORAI-specific blocker, however, showed impaired expression of RORγt in vitro and in vivo, while *Orai1*$^{-/-}$ T cells showed impaired differentiation of Th17 cells in vitro in one study (19), but not in an independent *Orai1* KO mouse model (34). It is possible that ORAI blocker can have a more substantial effect than deletion of *Orai1* because it can inhibit all the ORAI family members, including ORAI1, ORAI2, and ORAI3. Also, differences in genetic backgrounds of *Orai1* KO mice (mixed vs. C57BL/6) and deletion strategy (global vs. conditional) may yield altered outcomes. Not much is known about the roles of ORAI and STIM proteins in pathogenicity of Th17 cells. However, it was shown that loss of STIM1 influences the function of pathogenic Th17 cells and anti-fungal non-pathogenic Th17 cells by influencing oxidative phosphorylation or anaerobic glycolysis (35, 36). These studies showed that expression of RORγt was reduced in pathogenic Th17 cells but was not changed in non-pathogenic Th17 cells by loss of STIM1. These observations collectively suggest that SOCE mediated by ORAI1 and STIM1 has a relatively minor role in the initial event of Th17 differentiation, including expression of RORγt and RORα, but rather is essential for the maintenance (e.g., IL-23R) and terminal effector functions (e.g., IL-17 production). Also, SOCE seems to be essential for the functions of both pathogenic and protective, non-pathogenic Th17 cells. Based on the current data, it is likely that NKD2, an important regulator of CRAC channels but not essential components like ORAI1 and STIM1, plays a more selective role in distinct Th17 subsets.

Author Manuscript Author Manuscript Author Manuscript Author Manuscript

In a previous study, we identified CRACR2a as an essential regulator for CRAC channels (15, 16). Similar to NKD2, CRACR2a is expressed at high levels in effector T cells, and its deletion selectively blocks Th1 and Th17 responses only in the inflamed tissues without influencing T cell development in the thymus, homeostasis in the peripheral lymphoid organs, and the priming of T cells in the lymph nodes after immunization (17). However, unlike NKD2, deletion of *Cracr2a* predominantly impairs Th1 responses. *Cracr2a*$^{-/-}$ T cells showed reduced expression of the signature transcription factor, T-bet, suggesting its involvement in the early phase of Th1 polarization. *Cracr2a*$^{-/-}$ T cells cultured under pathogenic Th17-polarizing conditions (IL-6 + TGF-β + IL-23) produced normal levels of IL-17 but had defects in trans-differentiation into Th1-like T cells as judged by decreased expression of IFN-γ and T-bet after re-stimulation with IL-12. Although the phenotypes of *Cracr2a*$^{-/-}$ and *Nkd2*$^{-/-}$ T cells display similarity in the phenotypes in EAE, there are differences in molecular mechanisms. CRACR2a stabilizes ORAI1-STIM1 interaction by interacting with both proteins during the early events of CRAC channel activation (16, 17), whereas NKD2 regulates ORAI1^{+} vesicle trafficking by providing enough PM-resident ORAI1 from the intracellular pool, and hence essential for the sustained levels of Ca^{2+} entry. Furthermore, CRACR2a also influences c-Jun N-terminal kinase (JNK) signaling, crucial for Th1 differentiation, which is unaffected due to loss of NKD2. Therefore, it is possible that CRACR2a regulates the early phase of Ca^{2+} and JNK signaling pathways that influences expression of both signature transcription factors and cytokines, whereas NKD2 is essential for the late events of effector T cells, including cytokine expression, maintenance, and trans-differentiation by regulating sustained SOCE. Regardless, pathogenic effector T cells seem to be equipped with various molecular mechanisms to support robust transient and sustained Ca^{2+} entry.

In conclusion, although it is generally accepted that Ca^{2+} signaling influences various phases of T cell activation, the current study suggests that the pathogenic state of effector T cells requires exquisitely high and sustained intracellular Ca^{2+} elevation. NKD2 appears to be a regulator for CRAC channels, which impacts the pathogenicity of Th1 and Th17 cells by inducing inflammatory cytokines, including IFN-γ, IL-17, and GM-CSF. Intracellular Ca^{2+} elevation by NKD2 also promotes trans-differentiation of Th17 cells to Th1-like cells by inducing expression of transcription factors involved in Th17 pathogenicity (e.g., T-bet). Hence, the current data showed that pathogenic Th17 cells develop a unique strategy to suffice their need for sustained intracellular Ca^{2+} levels via utilizing the additional pool of intracellular ORAI1 in an NKD2-dependent manner. The *Drosophila* Nkd protein guides embryonic development by regulating a gradient of Wnt/β-catenin signaling across each segmental anlage (37). However, deletion of *Nkd* in mice did not influence viability and fertility, suggesting that the function of NKD proteins is dispensable for embryonic development (21). The current work shows that NKD2 plays a specialized role in effector T cells of mice and humans. *NKD2* gene, located on chromosome 5, has been linked to various human diseases, including asthma, Crohn's disease, and multiple sclerosis, based on genome-wide association studies (38-42). Therefore, understanding the function of NKD2 in T cells may reveal how its variations link to immune-related diseases and provide potential therapeutic targets for suppressing T cell-mediated autoimmune diseases.

Author Manuscript Author Manuscript Author Manuscript Author Manuscript

Supplementary Material

Refer to Web version on PubMed Central for supplementary material.

Acknowledgments

Flow cytometry was performed in the UCLA Jonsson Comprehensive Cancer Center (JCCC) and Center for AIDS Research Flow Cytometry Core Facility that is supported by National Institutes of Health awards P30 CA016042 and 5P30 AI028697, and by the JCCC, the UCLA AIDS Institute, the David Geffen School of Medicine at UCLA, the UCLA Chancellor's Office, and the UCLA Vice Chancellor's Office of Research. This work was supported by the National Institute of Health grants AI083432, AI146615, AI147063, and AI149236 (Y.G.) and AI130653 and AI146352 (S.S).

References

1. Lewis RS 2011. Store-operated calcium channels: new perspectives on mechanism and function. Cold Spring Harb Perspect Biol 3.
2. Srikanth S, and Gwack Y. 2013. Orai1-NFAT signalling pathway triggered by T cell receptor stimulation. Mol Cells 35: 182–194. [PubMed: 23483280]
3. Yu F, Sun L, and Machaca K. 2009. Orai1 internalization and STIM1 clustering inhibition modulate SOCE inactivation during meiosis. Proc Natl Acad Sci U S A 106: 17401–17406. [PubMed: 19805124]
4. Yu F, Sun L, and Machaca K. 2010. Constitutive recycling of the store-operated Ca2+ channel Orai1 and its internalization during meiosis. J Cell Biol 191: 523–535. [PubMed: 21041445]
5. Hodeify R, Selvaraj S, Wen J, Arredouani A, Hubrack S, Dib M, Al-Thani SN, McGraw T, and Machaca K. 2015. A STIM1-dependent 'trafficking trap' mechanism regulates Orai1 plasma membrane residence and Ca(2)(+) influx levels. J Cell Sci 128: 3143–3154. [PubMed: 26116575]
6. Wu B, Woo JS, Vila P, Jew M, Leung J, Sun Z, Srikanth S, and Gwack Y. 2021. NKD2 mediates stimulation-dependent ORAI1 trafficking to augment Ca(2+) entry in T cells. Cell Rep 36: 109603. [PubMed: 34433025]
7. Goverman J 2009. Autoimmune T cell responses in the central nervous system. Nat Rev Immunol 9: 393–407. [PubMed: 19444307]
8. Hirota K, Duarte JH, Veldhoen M, Hornsby E, Li Y, Cua DJ, Ahlfors H, Wilhelm C, Tolaini M, Menzel U, Garefalaki A, Potocnik AJ, and Stockinger B. 2011. Fate mapping of IL-17-producing T cells in inflammatory responses. Nat Immunol 12: 255–263. [PubMed: 21278737]
9. Kebir H, Ifergan I, Alvarez JI, Bernard M, Poirier J, Arbour N, Duquette P, and Prat A. 2009. Preferential recruitment of interferon-gamma-expressing TH17 cells in multiple sclerosis. Ann Neurol 66: 390–402. [PubMed: 19810097]
10. El-Behi M, Ciric B, Dai H, Yan Y, Cullimore M, Safavi F, Zhang GX, Dittel BN, and Rostami A. 2011. The encephalitogenicity of T(H)17 cells is dependent on IL-1- and IL-23-induced production of the cytokine GM-CSF. Nat Immunol 12: 568–575. [PubMed: 21516111]
11. Codarri L, Gyulveszi G, Tosevski V, Hesske L, Fontana A, Magnenat L, Suter T, and Becher B. 2011. RORgammat drives production of the cytokine GM-CSF in helper T cells, which is essential for the effector phase of autoimmune neuroinflammation. Nat Immunol 12: 560–567. [PubMed: 21516112]
12. Wang Y, Godec J, Ben-Aissa K, Cui K, Zhao K, Pucsek AB, Lee YK, Weaver CT, Yagi R, and Lazarevic V. 2014. The Transcription Factors T-bet and Runx Are Required for the Ontogeny of Pathogenic Interferon-gamma-Producing T Helper 17 Cells. Immunity 40: 355–366. [PubMed: 24530058]
13. Karmaus PWF, Chen X, Lim SA, Herrada AA, Nguyen TM, Xu B, Dhungana Y, Rankin S, Chen W, Rosencrance C, Yang K, Fan Y, Cheng Y, Easton J, Neale G, Vogel P, and Chi H. 2019. Metabolic heterogeneity underlies reciprocal fates of TH17 cell stemness and plasticity. Nature 565: 101–105. [PubMed: 30568299]
14. Lee JY, Hall JA, Kroehling L, Wu L, Najar T, Nguyen HH, Lin WY, Yeung ST, Silva HM, Li D, Hine A, Loke P, Hudesman D, Martin JC, Kenigsberg E, Merad M, Khanna KM, and Littman

Author Manuscript Author Manuscript Author Manuscript Author Manuscript

DR. 2020. Serum Amyloid A Proteins Induce Pathogenic Th17 Cells and Promote Inflammatory Disease. Cell 180: 79–91 e16. [PubMed: 31866067]

15. Srikanth S, Jung HJ, Kim KD, Souda P, Whitelegge J, and Gwack Y. 2010. A novel EF-hand protein, CRACR2A, is a cytosolic Ca2+ sensor that stabilizes CRAC channels in T cells. Nat Cell Biol 12: 436–446. [PubMed: 20418871]
16. Srikanth S, Kim KD, Gao Y, Woo JS, Ghosh S, Calmettes G, Paz A, Abramson J, Jiang M, and Gwack Y. 2016. A large Rab GTPase encoded by CRACR2A is a component of subsynaptic vesicles that transmit T cell activation signals. Sci Signal 9: ra31. [PubMed: 27016526]
17. Woo JS, Srikanth S, Kim KD, Elsaesser H, Lu J, Pellegrini M, Brooks DG, Sun Z, and Gwack Y. 2018. CRACR2A-Mediated TCR Signaling Promotes Local Effector Th1 and Th17 Responses. J Immunol 201: 1174–1185. [PubMed: 29987160]
18. Srikanth S, Jung HJ, Ribalet B, and Gwack Y. 2010. The intracellular loop of Orai1 plays a central role in fast inactivation of Ca2+ release-activated Ca2+ channels. J Biol Chem 285: 5066–5075. [PubMed: 20007711]
19. Kim KD, Srikanth S, Tan YV, Yee MK, Jew M, Damoiseaux R, Jung ME, Shimizu S, An DS, Ribalet B, Waschek JA, and Gwack Y. 2014. Calcium Signaling via Orai1 Is Essential for Induction of the Nuclear Orphan Receptor Pathway To Drive Th17 Differentiation. J Immunol 192: 110–122. [PubMed: 24307733]
20. He Z, Ma J, Wang R, Zhang J, Huang Z, Wang F, Sen S, Rothenberg EV, and Sun Z. 2017. A two-amino-acid substitution in the transcription factor RORgammat disrupts its function in TH17 differentiation but not in thymocyte development. Nat Immunol 18: 1128–1138. [PubMed: 28846085]
21. Zhang S, Cagatay T, Amanai M, Zhang M, Kline J, Castrillon DH, Ashfaq R, Oz OK, and Wharton KA Jr. 2007. Viable mice with compound mutations in the Wnt/Dvl pathway antagonists nkd1 and nkd2. Mol Cell Biol 27: 4454–4464. [PubMed: 17438140]
22. Gaublomme JT, Yosef N, Lee Y, Gertner RS, Yang LV, Wu C, Pandolfi PP, Mak T, Satija R, Shalek AK, Kuchroo VK, Park H, and Regev A. 2015. Single-Cell Genomics Unveils Critical Regulators of Th17 Cell Pathogenicity. Cell 163: 1400–1412. [PubMed: 26607794]
23. Ghoreschi K, Laurence A, Yang XP, Tato CM, McGeachy MJ, Konkel JE, Ramos HL, Wei L, Davidson TS, Bouladoux N, Grainger JR, Chen Q, Kanno Y, Watford WT, Sun HW, Eberl G, Shevach EM, Belkaid Y, Cua DJ, Chen W, and O'Shea JJ. 2010. Generation of pathogenic T(H)17 cells in the absence of TGF-beta signalling. Nature 467: 967–971. [PubMed: 20962846]
24. Lee Y, Awasthi A, Yosef N, Quintana FJ, Xiao S, Peters A, Wu C, Kleinewietfeld M, Kunder S, Hafler DA, Sobel RA, Regev A, and Kuchroo VK. 2012. Induction and molecular signature of pathogenic TH17 cells. Nat Immunol 13: 991–999. [PubMed: 22961052]
25. Ivanov II, McKenzie BS, Zhou L, Tadokoro CE, Lepelley A, Lafaille JJ, Cua DJ, and Littman DR. 2006. The orphan nuclear receptor RORgammat directs the differentiation program of proinflammatory IL-17+ T helper cells. Cell 126: 1121–1133. [PubMed: 16990136]
26. Yang XO, Pappu BP, Nurieva R, Akimzhanov A, Kang HS, Chung Y, Ma L, Shah B, Panopoulos AD, Schluns KS, Watowich SS, Tian Q, Jetten AM, and Dong C. 2008. T helper 17 lineage differentiation is programmed by orphan nuclear receptors ROR alpha and ROR gamma. Immunity 28: 29–39. [PubMed: 18164222]
27. Lee YK, Turner H, Maynard CL, Oliver JR, Chen D, Elson CO, and Weaver CT. 2009. Late developmental plasticity in the T helper 17 lineage. Immunity 30: 92–107. [PubMed: 19119024]
28. Langrish CL, Chen Y, Blumenschein WM, Mattson J, Basham B, Sedgwick JD, McClanahan T, Kastelein RA, and Cua DJ. 2005. IL-23 drives a pathogenic T cell population that induces autoimmune inflammation. J Exp Med 201: 233–240. [PubMed: 15657292]
29. Muranski P, Borman ZA, Kerkar SP, Klebanoff CA, Ji Y, Sanchez-Perez L, Sukumar M, Reger RN, Yu Z, Kern SJ, Roychoudhuri R, Ferreyra GA, Shen W, Durum SK, Feigenbaum L, Palmer DC, Antony PA, Chan CC, Laurence A, Danner RL, Gattinoni L, and Restifo NP. 2011. Th17 cells are long lived and retain a stem cell-like molecular signature. Immunity 35: 972–985. [PubMed: 22177921]
30. Putney JW Jr., Broad LM, Braun FJ, Lievremont JP, and Bird GS. 2001. Mechanisms of capacitative calcium entry. J Cell Sci 114: 2223–2229. [PubMed: 11493662]

Author Manuscript Author Manuscript Author Manuscript Author Manuscript

31. Pawlak M, Ho AW, and Kuchroo VK. 2020. Cytokines and transcription factors in the differentiation of CD4(+) T helper cell subsets and induction of tissue inflammation and autoimmunity. Curr Opin Immunol 67: 57–67. [PubMed: 33039897]
32. Honda K, and Littman DR. 2016. The microbiota in adaptive immune homeostasis and disease. Nature 535: 75–84. [PubMed: 27383982]
33. Ma J, McCarl CA, Khalil S, Luthy K, and Feske S. 2010. T-cell-specific deletion of STIM1 and STIM2 protects mice from EAE by impairing the effector functions of Th1 and Th17 cells. Eur J Immunol 40: 3028–3042. [PubMed: 21061435]
34. Kaufmann U, Shaw PJ, Kozhaya L, Subramanian R, Gaida K, Unutmaz D, McBride HJ, and Feske S. 2016. Selective ORAI1 Inhibition Ameliorates Autoimmune Central Nervous System Inflammation by Suppressing Effector but Not Regulatory T Cell Function. J Immunol 196: 573–585. [PubMed: 26673135]
35. Kaufmann U, Kahlfuss S, Yang J, Ivanova E, Koralov SB, and Feske S. 2019. Calcium Signaling Controls Pathogenic Th17 Cell-Mediated Inflammation by Regulating Mitochondrial Function. Cell Metab 29: 1104–1118 e1106. [PubMed: 30773462]
36. Kahlfuss S, Kaufmann U, Concepcion AR, Noyer L, Raphael D, Vaeth M, Yang J, Pancholi P, Maus M, Muller J, Kozhaya L, Khodadadi-Jamayran A, Sun Z, Shaw P, Unutmaz D, Stathopulos PB, Feist C, Cameron SB, Turvey SE, and Feske S. 2020. STIM1-mediated calcium influx controls antifungal immunity and the metabolic function of non-pathogenic Th17 cells. EMBO Mol Med 12: e11592. [PubMed: 32609955]
37. Zeng W, Wharton KA Jr., Mack JA, Wang K, Gadbaw M, Suyama K, Klein PS, and Scott MP. 2000. naked cuticle encodes an inducible antagonist of Wnt signalling. Nature 403: 789–795. [PubMed: 10693810]
38. Hindorff LA, Sethupathy P, Junkins HA, Ramos EM, Mehta JP, Collins FS, and Manolio TA. 2009. Potential etiologic and functional implications of genome-wide association loci for human diseases and traits. Proc Natl Acad Sci U S A 106: 9362–9367. [PubMed: 19474294]
39. Baranzini SE, Srinivasan R, Khankhanian P, Okuda DT, Nelson SJ, Matthews PM, Hauser SL, Oksenberg JR, and Pelletier D. 2010. Genetic variation influences glutamate concentrations in brains of patients with multiple sclerosis. Brain 133: 2603–2611. [PubMed: 20802204]
40. Franke A, McGovern DP, Barrett JC, Wang K, Radford-Smith GL, Ahmad T, Lees CW, Balschun T, Lee J, Roberts R, Anderson CA, Bis JC, Bumpstead S, Ellinghaus D, Festen EM, Georges M, Green T, Haritunians T, Jostins L, Latiano A, Mathew CG, Montgomery GW, Prescott NJ, Raychaudhuri S, Rotter JI, Schumm P, Sharma Y, Simms LA, Taylor KD, Whiteman D, Wijmenga C, Baldassano RN, Barclay M, Bayless TM, Brand S, Buning C, Cohen A, Colombel JF, Cottone M, Stronati L, Denson T, De Vos M, D'Inca R, Dubinsky M, Edwards C, Florin T, Franchimont D, Gearry R, Glas J, Van Gossum A, Guthery SL, Halfvarson J, Verspaget HW, Hugot JP, Karban A, Laukens D, Lawrance I, Lemann M, Levine A, Libioulle C, Louis E, Mowat C, Newman W, Panes J, Phillips A, Proctor DD, Regueiro M, Russell R, Rutgeerts P, Sanderson J, Sans M, Seibold F, Steinhart AH, Stokkers PC, Torkvist L, Kullak-Ublick G, Wilson D, Walters T, Targan SR, Brant SR, Rioux JD, D'Amato M, Weersma RK, Kugathasan S, Griffiths AM, Mansfield JC, Vermeire S, Duerr RH, Silverberg MS, Satsangi J, Schreiber S, Cho JH, Annese V, Hakonarson H, Daly MJ, and Parkes M. 2010. Genome-wide meta-analysis increases to 71 the number of confirmed Crohn's disease susceptibility loci. Nat Genet 42: 1118–1125. [PubMed: 21102463]
41. Moffatt MF, Gut IG, Demenais F, Strachan DP, Bouzigon E, Heath S, von Mutius E, Farrall M, Lathrop M, Cookson W, and G. Consortium. 2010. A large-scale, consortium-based genomewide association study of asthma. N Engl J Med 363: 1211–1221. [PubMed: 20860503]
42. Ahola-Olli AV, Wurtz P, Havulinna AS, Aalto K, Pitkanen N, Lehtimaki T, Kahonen M, Lyytikainen LP, Raitoharju E, Seppala I, Sarin AP, Ripatti S, Palotie A, Perola M, Viikari JS, Jalkanen S, Maksimow M, Salomaa V, Salmi M, Kettunen J, and Raitakari OT. 2017. Genome-wide Association Study Identifies 27 Loci Influencing Concentrations of Circulating Cytokines and Growth Factors. Am J Hum Genet 100: 40–50. [PubMed: 27989323]

Author Manuscript Author Manuscript Author Manuscript Author Manuscript

Key Points

- Pathogenic Th17 cells show higher ORAI1-dependent SOCE than non-pathogenic Th17 cells
- NKD2 is important for sustained ORAI1-dependent SOCE in pathogenic Th17 cells

Author Manuscript Author Manuscript Author Manuscript Author Manuscript

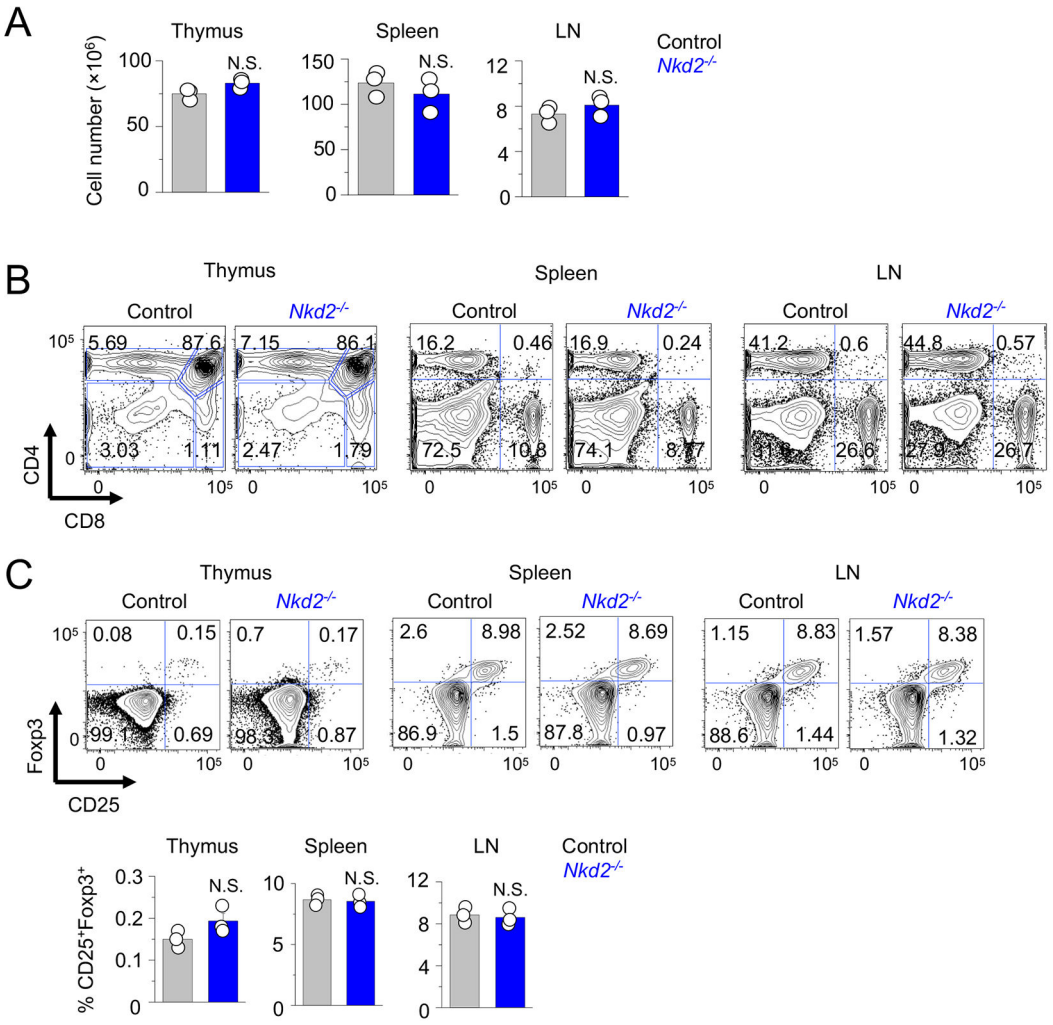

Figure 1. Loss of NKD2 does not affect T cell development and homeostasis

(**A**) Total cell numbers from thymi, spleen, and lymph nodes (LN) of control and *Nkd2*$^{-/-}$ mice.

(**B**) Representative flow plots showing the frequency of CD4^{+} and CD8^{+} T cell populations from lymphoid organs of control or *Nkd2*$^{-/-}$ mice. Data are representative of three independent pairs of animals.

(**C**) Representative flow plots (top) showing the frequency of CD25^{+}Foxp3^{+} T cells among CD4^{+} T cell populations from the thymi, spleen, and lymph nodes of control and *Nkd2*$^{-/-}$ mice. The bar graphs (bottom) showing averaged frequencies (± s.e.m.) of CD25^{+}Foxp3^{+} T cells. Data are representative of three independent pairs of animals.

In panels (**A**) and (**C**), each symbol represents data from an independent animal. N.S., not significant.

Author Manuscript Author Manuscript Author Manuscript Author Manuscript

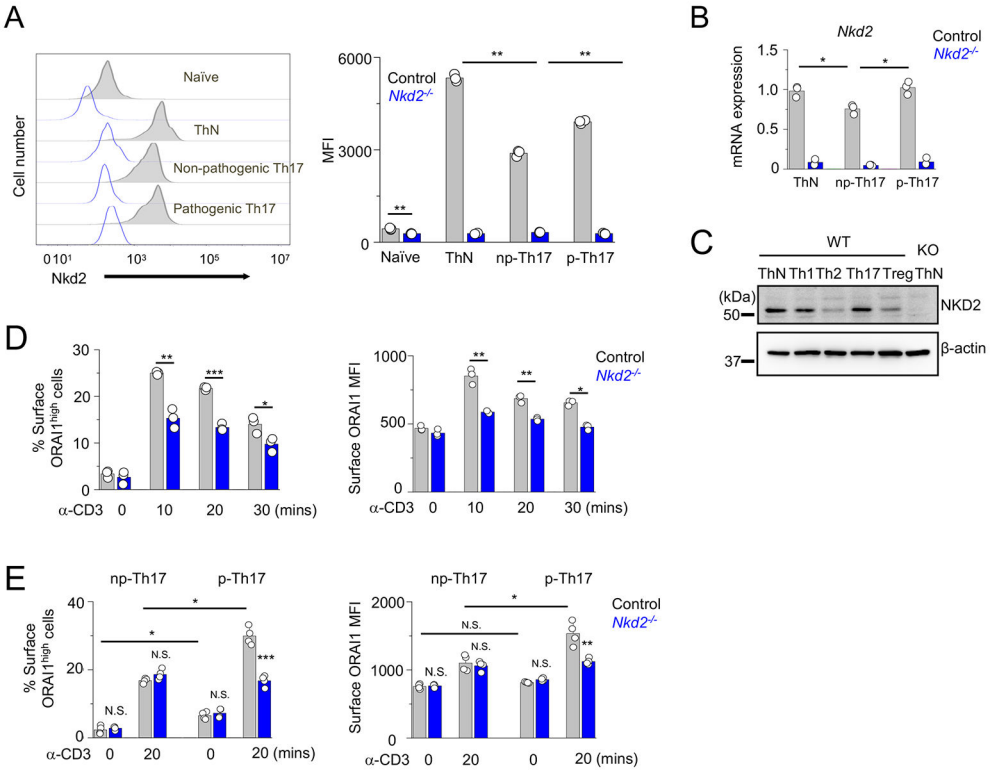

Figure 2. NKD2 is abundantly expressed in Th1 cells and those polarized under pathogenic Th17-polarizing conditions

(**A**) Representative histogram showing NKD2 expression in naïve and effector T cells cultured under non-polarizing (ThN), non-pathogenic Th17-polarizing (np-Th17), and pathogenic Th17-polarizing (p-Th17) conditions (left). *Nkd2*$^{-/-}$ T cells (open blue histograms) were used as a negative control for staining. The bar graph (right) shows average mean fluorescence intensities (MFIs ± s.e.m.) of NKD2^{+} population. Each symbol represents data from an independent staining.

(**B**) Control and *Nkd2*$^{-/-}$ naïve T cells were cultured under non-polarizing conditions or under non-pathogenic or pathogenic Th17-polarizing conditions (see methods for details). Four days after differentiation, cells were harvested for transcript analysis of *Nkd2*. Data show representative triplicates from two independent experiments.

(**C**) Representative immunoblot showing NKD2 expression in lysates of primary murine effector T cells of indicated lineages. Lysates of *Nkd2*$^{-/-}$ cells were loaded to show specificity of the antibody. β-actin - loading control. Th17 – T cells cultured under pathogenic Th17-polarizing conditions.

(**D**) Control and *Nkd2*$^{-/-}$ T cells were differentiated under non-polarizing conditions and transduced to express ORAI1-EC-HA that contains an HA tag in the extracellular domain. Cells were stained with anti-HA antibodies without permeabilization to label plasma membrane-localized ORAI1 at indicated time points after TCR stimulation. Data shows the average (± s.e.m.) frequencies (left) or MFIs (right) from three independent experiments.

(**E**) Control and *Nkd2*$^{-/-}$ T cells cultured under non-pathogenic or pathogenic Th17-polarizing conditions and transduced to express ORAI1-EC-HA were stained with anti-HA antibodies without permeabilization to label plasma membrane-localized ORAI1 at indicated

Author Manuscript Author Manuscript Author Manuscript Author Manuscript

time points after TCR stimulation. Data shows average (± s.e.m.) frequencies (left) or MFIs (right) from three independent experiments.
* $p<0.05$, ** $p<0.005$, *** $p<0.0001$.

Author Manuscript Author Manuscript Author Manuscript Author Manuscript

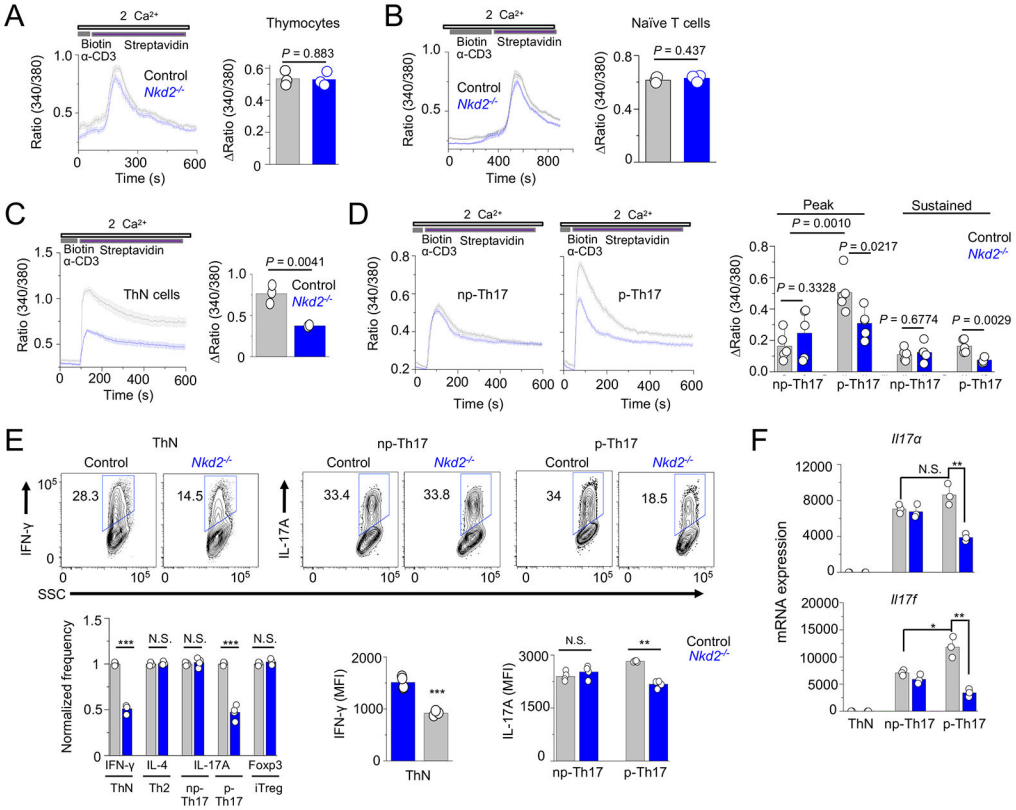

Figure 3. Loss of *Nkd2* impairs store-operated Ca^{2+} entry and cytokine production in effector T cells

(**A**) Representative traces showing averaged SOCE from control or *Nkd2*$^{-/-}$ (N = 54 for control and 63 cells for *Nkd2*$^{-/-}$) thymocytes after TCR cross-linking using biotin-tagged anti-CD3 antibodies (2.5 μg/ml) and streptavidin (10 μg/ml) in the presence of external solution containing 2 mM Ca^{2+}. Bar graphs show averaged baseline-subtracted SOCE (± s.e.m.) at the peak from three independent experiments.

(**B**) Representative traces showing averaged SOCE from control or *Nkd2*$^{-/-}$ naïve T cells (N = 72 for control and 71 cells for *Nkd2*$^{-/-}$) after TCR cross-linking. Bar graphs show averaged baseline-subtracted SOCE (± s.e.m.) at the peak from three independent experiments.

(**C**) Representative traces showing averaged SOCE from control or *Nkd2*$^{-/-}$ ThN cells (N = 72 for control and 71 cells for *Nkd2*$^{-/-}$, right panel) after TCR cross-linking. Bar graphs show averaged baseline-subtracted SOCE (± s.e.m.) at the peak from three independent experiments.

(**D**) Representative traces showing averaged SOCE from control or *Nkd2*$^{-/-}$ T cells polarized under non-pathogenic (np-, N = 44 for control and 54 cells for *Nkd2*$^{-/-}$, left panel) or pathogenic (p-, N = 64 cells for both control and *Nkd2*$^{-/-}$, right panel) Th17-polarizing conditions after TCR cross-linking. Bar graphs show averaged baseline-subtracted SOCE (± s.e.m.) at the peak and later time point (600 second, sustained) from 4-5 independent experiments.

(**E**) Representative flow plots showing expression of IFN-γ (ThN cells) and IL-17A (T cells polarized under non-pathogenic or pathogenic Th17-polarizing conditions) in control

Author Manuscript Author Manuscript Author Manuscript Author Manuscript

and *Nkd2*$^{-/-}$ effector T cells after re-stimulation with anti-CD3 and anti-CD28 antibodies for 5 hours on day 4. Bar graphs below shows normalized frequencies (average ± s.e.m.) and MFIs of indicated cytokines as pooled technical replicates from three independent experiments.

(**F**) Relative expression of indicated genes in control and *Nkd2*$^{-/-}$ T cells cultured under non-polarizing conditions or under non-pathogenic or pathogenic Th17-polarizing conditions. Cells were cultured for 4 days and restimulated before harvesting for transcript analysis. Data shows one representative triplicate from two independent experiments.

In panels A-E each symbol represents data obtained from an independent pair of control and *Nkd2*$^{-/-}$ animals. N.S., not significant; *** $p<0.0001$.

Author Manuscript Author Manuscript Author Manuscript Author Manuscript

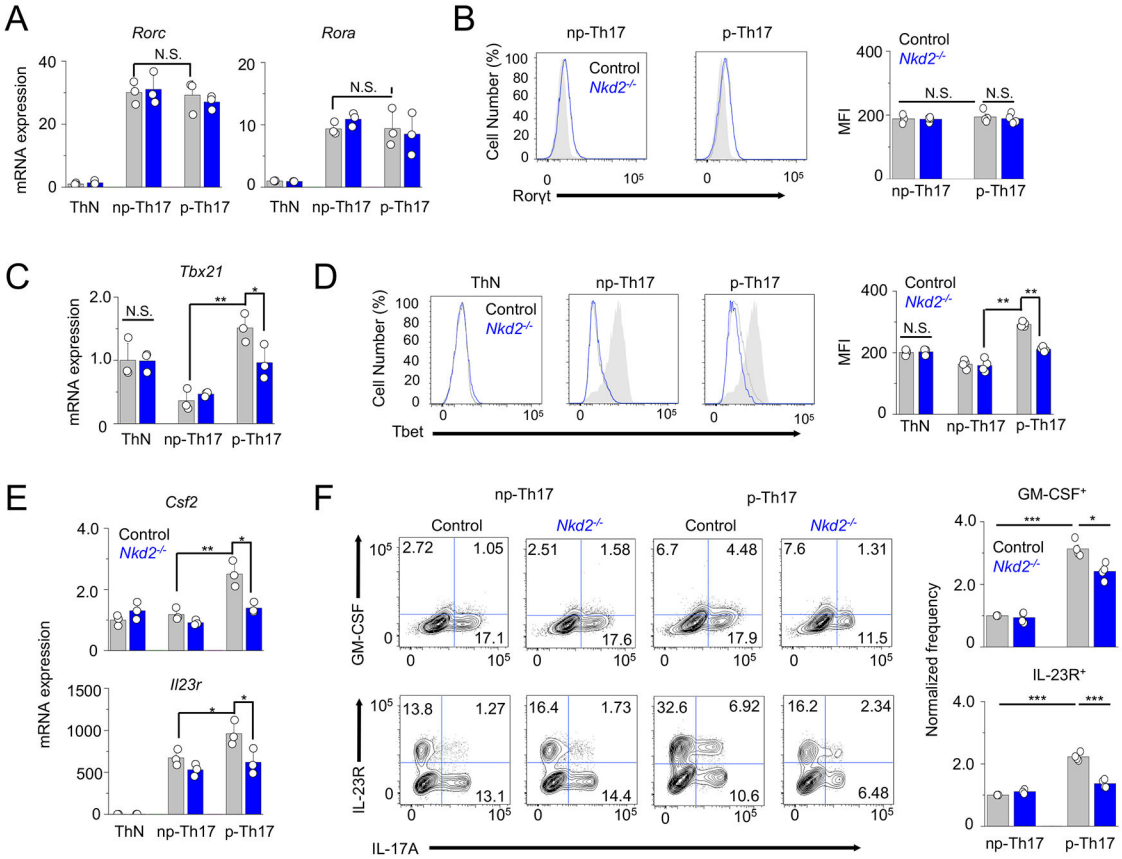

Figure 4. Loss of Nkd2 decreases the expression of genes involved in Th17 pathogenicity

(**A**) Relative expression of indicated genes in control and *Nkd2*$^{-/-}$ T cells cultured under non-polarizing conditions or under non-pathogenic or pathogenic Th17-polarizing conditions.

(**B**) Representative flow plots showing expression of RORγt in control and *Nkd2*$^{-/-}$ T cells differentiated under non-pathogenic or pathogenic Th17-polarizing conditions. Th1 cells (gray) were used as negative controls. The bar graphs show the average (± s.e.m.) frequencies and MFIs from four independent experiments.

(**C**) Relative expression of indicated genes in control and *Nkd2*$^{-/-}$ T cells cultured under non-polarizing conditions or under non-pathogenic or pathogenic Th17-polarizing conditions.

(**D**) Representative flow plots showing expression of T-bet in control and *Nkd2*$^{-/-}$ T cells differentiated under non-pathogenic or pathogenic Th17-polarizing conditions. Th1 cells (gray) were used as positive control. The bar graphs below show the average (± s.e.m.) frequencies and MFIs from four independent experiments.

(**E**) Relative expression of indicated genes in control and *Nkd2*$^{-/-}$ T cells cultured under non-polarizing conditions or under non-pathogenic or pathogenic Th17-polarizing conditions.

(**F**) Representative flow plots showing the expression of indicated cytokines and cytokine receptors in control and *Nkd2*$^{-/-}$ T cells cultured under non-pathogenic or pathogenic Th17-

Author Manuscript Author Manuscript Author Manuscript Author Manuscript

polarizing conditions. Cells were re-stimulated with anti-CD3 and anti-CD28 antibodies on day 4. Bar graphs show averages (± s.e.m.) from four independent experiments.
In panels (**A**), (**C**), and (**E**), cells were cultured for four days and restimulated before harvesting for transcript analysis. Data shows one representative triplicate from two independent experiments. N.S., not significant; * $p<0.05$, ** $p<0.005$, *** $p<0.0001$

Author Manuscript Author Manuscript Author Manuscript Author Manuscript

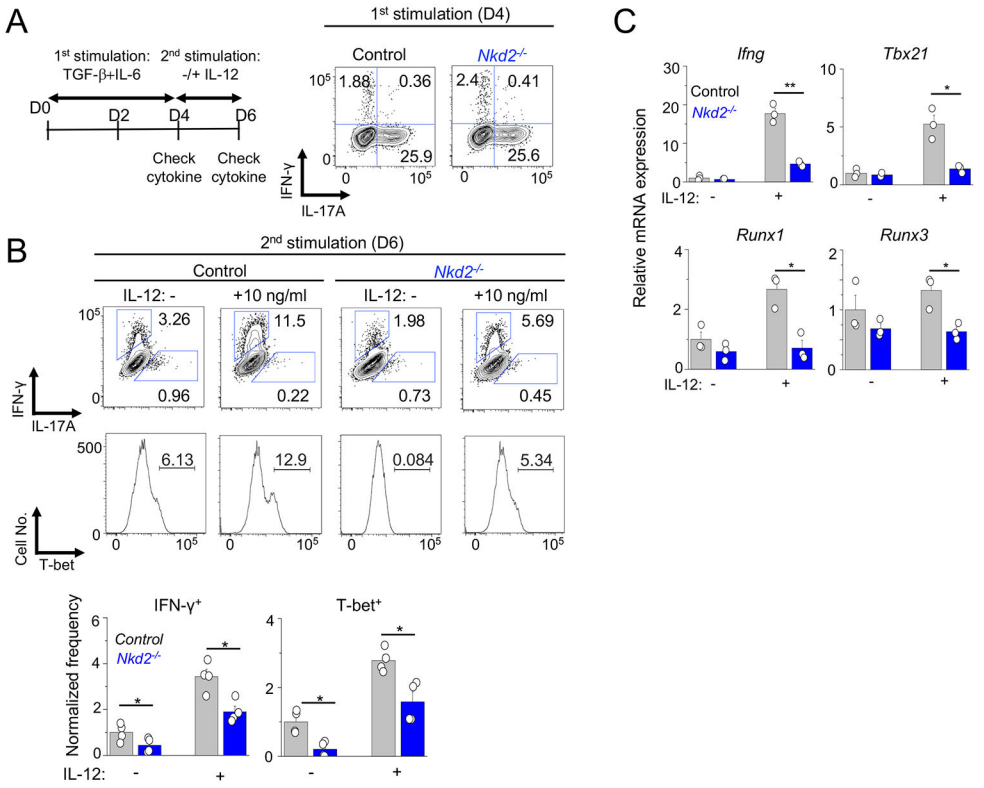

Figure 5. Loss of NKD2 impairs trans-differentiation of Th17 cells into IFN-γ producing cells

(**A**) Left - Schematic of the experimental design for trans-differentiation of Th17 cells. Right - Representative flow plots showing cytokine expression profile of control and *Nkd2*$^{-/-}$ cells cultured under non-pathogenic Th17-polarizing conditions for four days and re-stimulated with PMA plus ionomycin.

(**B**) Representative flow plots showing cytokine (top) or T-bet (bottom) expression in control and *Nkd2*$^{-/-}$ cells. Cells cultured under non-pathogenic Th17-polarizing conditions were re-stimulated with anti-CD3 and anti-CD28 antibodies in the presence or absence of IL-12. The bar graphs below show average (± s.e.m.) from four independent experiments.

(**C**) Transcript analysis of indicated genes in cells obtained from (B) after re-stimulation. Data show representative triplicates from two independent experiments.

* $p<0.05$, ** $p<0.005$.

Author Manuscript Author Manuscript Author Manuscript Author Manuscript

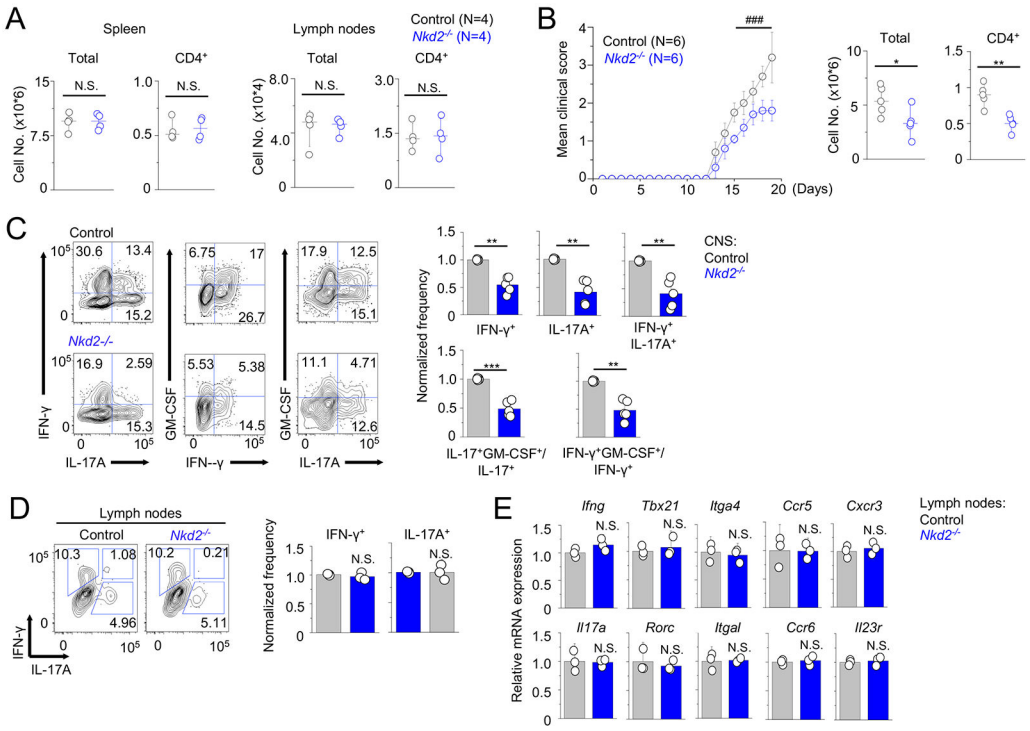

Figure 6. Loss of *Nkd2* impairs EAE pathogenesis after adoptive transfer of naïve T cells

(**A**) Total and CD4$^+$ T cell numbers in spleen and lymph nodes of *Rag2*$^{-/-}$ recipients of control or *Nkd2*$^{-/-}$ naïve T cells, two weeks post transfer.

(**B**) Time course of the mean clinical score of EAE in *Rag2*$^{-/-}$ recipients of control or *Nkd2*$^{-/-}$ naïve T cells. Mice were immunized with MOG peptide two weeks post transfer. The graph shows mean ± s.e.m. from two independent experiments (N = 8). Scatter plots show the numbers of total mononuclear (left) or CD4$^+$ T cells (right) isolated from the CNS of recipients at the peak of the disease (N = 5).

(**C**) Representative flow plots showing cytokine profile of CD4$^+$ T cells from the CNS of *Rag2*$^{-/-}$ recipients of control or *Nkd2*$^{-/-}$ naïve T cells at the peak of the disease. Bar graphs (right) show average (± s.e.m.) of normalized frequency of IFN-γ^+, IL-17A$^+$, and IFN-γ^+IL-17A$^+$ double-positive cells (top) and ratio of IL-17$^+$GM-CSF$^+$/IL-17$^+$ and IFN-γ^+GM-CSF$^+$/IFN-γ^+ cells (bottom). The frequencies and ratio values of CNS cells from recipients of *Nkd2*$^{-/-}$ cells were normalized to those of control cells.

(**D**) Representative flow plots showing expression of indicated cytokines from CD4$^+$ cells harvested from the draining lymph nodes of EAE-induced control and *Nkd2*$^{-/-}$ mice. Cells were harvested at the early stages of disease onset (score of <1.0) and stimulated with PMA plus ionomycin for 5 hours before cytokine staining. The bar graphs on the right show the averages of normalized frequencies (± s.e.m.) from three independent mice.

(**E**) Transcript analysis of indicated genes from cells harvested from the draining lymph nodes of control and *Nkd2*$^{-/-}$ mice at day 10 after EAE induction. Data show representative technical triplicates from two independent experiments.

In all the panels, each symbol represents data obtained from an independent mouse. Statistical significance for the clinical score in panel (**A**) was calculated using the Mann-

Whitney U test. ### p<0.0001. Other panels - Student's t test * p<0.05, ** p<0.005, *** p<0.0001, N.S., not significant.

Author Manuscript Author Manuscript Author Manuscript Author Manuscript

Author Manuscript Author Manuscript Author Manuscript Author Manuscript

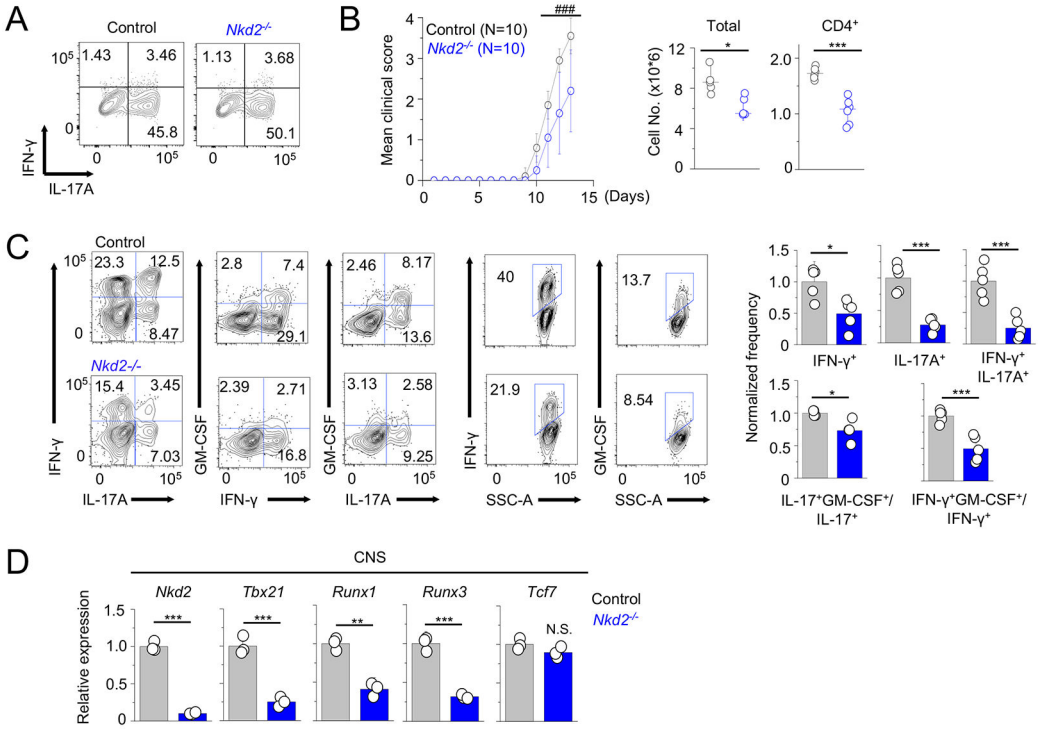

Figure 7. Loss of NKD2 impairs pathogenesis of effector T cell transfer-induced EAE

(**A**) Representative flow plots showing cytokine profile of CD4$^+$T cells from the draining lymph nodes of control or *Nkd2*$^{-/-}$ mice injected with MOG peptide for EAE induction, cultured under Th17 expansion conditions (with IL-1β + IL-23) for 72 hours, and stimulated with PMA plus ionomycin for 5 hours.

(**B**) Time course of the mean clinical score of EAE in *Rag2*$^{-/-}$ mice after adoptive transfer of control or *Nkd2*$^{-/-}$ draining lymph node cells cultured under Th17-expansion conditions. The line graph shows mean ± s.e.m. from the indicated number of animals pooled from three independent experiments. Scatter plots show the numbers of total mononuclear (left) or CD4$^+$ T cells (right) isolated from the CNS of recipients of control or *Nkd2*$^{-/-}$ cells at the peak of the disease.

(**C**) Representative flow plots showing the cytokine profile of CD4$^+$ T cells from the CNS of recipients of control or *Nkd2*$^{-/-}$ cells at the peak of the disease. Bar graphs (right) show average (± s.e.m.) of normalized frequency of IFN-γ$^+$, IL-17A$^+$, and IFN-γ$^+$IL-17A$^+$ double-positive cells (top) and ratio of IL-17$^+$GM-CSF$^+$/IL-17$^+$ and IFN-γ$^+$GM-CSF$^+$/IFN-γ$^+$ cells (bottom). The frequencies of CNS cells from recipients of *Nkd2*$^{-/-}$ cells were normalized to those of control T cells.

(**D**) Transcript analysis for expression (± s.e.m.) of the indicated genes in mononuclear cells isolated from the CNS of *Rag2*$^{-/-}$ recipients of control or *Nkd2*$^{-/-}$ cells at the peak of the disease.

In panels (**B**) - (**D**), each symbol represents data obtained from an independent animal. Statistical significance for the clinical score in panel (**B**) was calculated using the Mann-Whitney U test. $^{\#\#\#}$ p<0.0001. Other panels - Student's t test * p<0.05, ** p<0.005, *** p<0.0001.

Author Manuscript Author Manuscript Author Manuscript Author Manuscript

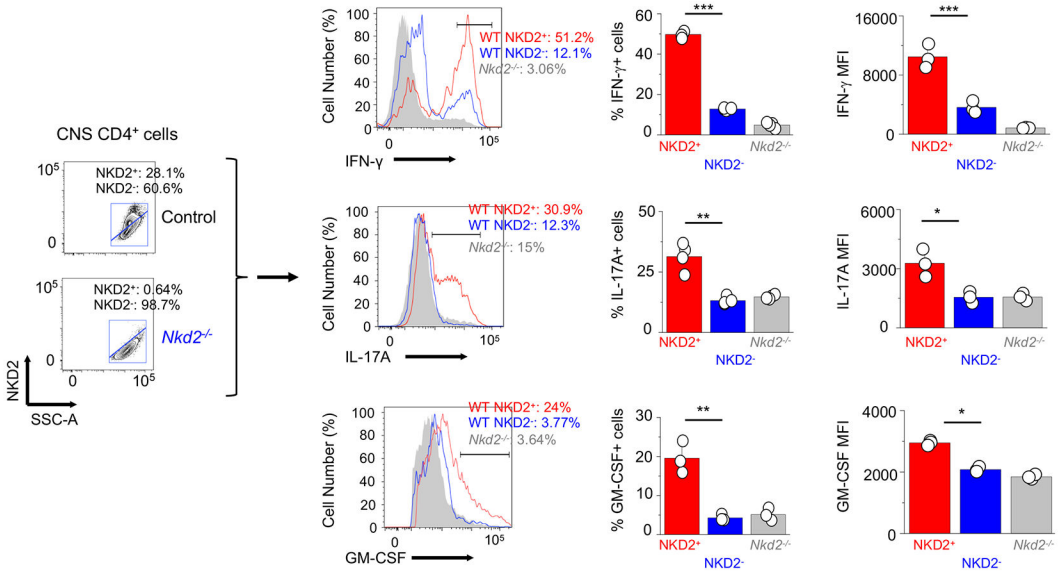

Figure 8. NKD2 expression correlates with increased cytokine production in effector T cells isolated from the central nervous system

Representative flow plots (left) showing NKD2 expression in $CD4^+$ cells isolated from the CNS of *Rag2*$^{-/-}$ recipients of control or *Nkd2*$^{-/-}$ T cells at the peak of the disease. Middle - Representative histograms showing frequencies of IFN-γ^+, IL-17A$^+$, or GM-CSF$^+$ population among NKD2$^+$ or NKD2$^-$ CD4$^+$ cells. Right - Bar graphs showing average frequencies (± s.e.m.) of cytokine production in NKD2$^+$ or NKD2$^-$ CD4$^+$ cells.

Each symbol represents data obtained from an independent animal. Student's t test * $p<0.05$, ** $p<0.005$, *** $p<0.0001$.